V64

Interferometry

Christopher Breitfeld
christopher.breitfeld@tu-dortmund.de

Henry Krämerkämper
henry.kraemerkaemper@tu-dortmund.de

Conducted: 18. December 2023 Submission: February 15, 2024

TU Dortmund – Fakultät Physik

Contents

1 Aims of the Experiment

The primary objective of this experiment is to ascertain the refractive indices of both glass and air. To achieve this, a Sagnac interferometer is employed. This device's design and operating principles enable precise measurement of refractive indices.

2 Theory

2.1 Interference of Coherent Light

Interference is a phenomenon where two waves superpose to form a resultant wave. This typically occurs when waves of compatible frequencies and phases converge, resulting in constructive or destructive interference patterns. A crucial requirement for observing clear interference patterns is *coherence*.

Coherence refers to a consistent phase relationship between the waves. It is distinguished into temporal and spatial coherence. Temporal coherence relates to the duration over which a wave's phase and amplitude remain predictable. Spatial coherence, on the other hand, refers to the uniformity of the light wave's phase across different areas of the wavefront. A laser beam, owing to its production process, exhibits high temporal and spatial coherence. The degree of coherence can be quantified as

$$\gamma_{1,2}(\vec{r}_1, t_1; \vec{r}_2, t_2) = \frac{\langle E(\vec{r}_1, t_1) E^*(\vec{r}_2, t_2) \rangle}{\sqrt{\langle |E(\vec{r}_1, t_1)|^2 \rangle \langle |E(\vec{r}_2, t_2)|^2 \rangle}} \tag{1}$$

where $E(\vec{r}_i, t_i)$ represents the amplitude of the electric field at position $\vec{r}_i$ and time t_i. A $\gamma_{1,2}$ value of 0 indicates complete incoherence, while 1 signifies perfect coherence.

Electromagnetic waves are transverse oscillations in the electromagnetic field, exhibiting different polarizations depending on their oscillation direction. Light can be polarized by passing through a polarization filter. Unpolarized light comprises multiple polarizations in various directions. A polarization filter allows only a specific polarization to pass through, effectively filtering out a single polarization from the unpolarized beam.

An alternative method for obtaining polarized light involves the use of a polarizing beam splitter cube (PBSC). This cube differentiates between s-polarized and p-polarized light: it reflects the s-polarized light, which oscillates perpendicular to the incidence plane and transmits the p-polarized light, oscillating parallel to this incidence plane.

While the degree of coherence, as defined in Equation (1), is a reliable measure for describing coherence, assessing the contrast of the interference pattern offers a more practical approach. The contrast, denoted by K, is defined as

$$K = \frac{I_{\max} - I_{\min}}{I_{\max} + I_{\min}}, \tag{2}$$

where $I_{\max}$ and $I_{\min}$ are the maximum and minimum intensities in the interference pattern. Analogous to the degree of coherence, K ranges from 0 to 1, with a perfect contrast represented by $K = 1$.

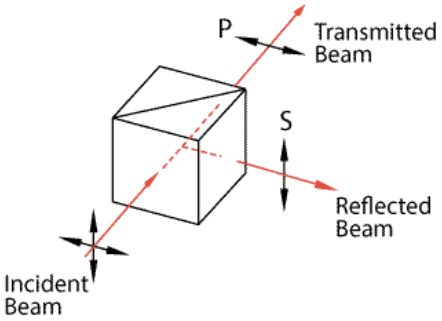

Figure 1: Schematic illustration of a Polarizing Beam Splitter Cube (PBSC). The cube divides an incident unpolarized beam into two components: one s-polarized and one p-polarized. [1]

Since the intensity I is proportional to the superposition of two waves, expressed as

$$I \propto \langle |E_1 \cos(\omega t) + E_2 \cos(\omega t + \delta)|^2 \rangle \tag{3}$$

where ω is the wave frequency and δ represents the phase difference between the two waves. Consequently, the maximal and minimal intensities can be written as

$$I_{\text{max/min}} \propto \frac{1}{2}(E_1^2 + E_2^2) \pm E_1 E_2.$$

The electric field depends on the polarization angle ϕ of the incoming beam, given by

$$E_1 = \sqrt{E_1 + E_2}\cos(\phi)$$
$$E_2 = \sqrt{E_1 + E_2}\sin(\phi).$$

Substituting these into the intensity equation (3) yields

$$I_{\text{max/min}} \propto (1 \pm 2\sin(\phi)\cos(\phi)).$$

Therefore, the contrast K, as defined in Equation (2), can be expressed as a function of the initial polarization angle ϕ:

$$K = 2|\sin(\phi)\cos(\phi)| \tag{4}$$

2.2 Refraction Indices of Glass and Gases

The refractive index, denoted as n, characterizes how the speed of light in a medium v compares to its speed in a vacuum c. Mathematically, it is expressed as

$$n = \frac{v}{c}.$$

Due to the change in light speed upon entering a medium with a different refractive index, a path length difference arises for a beam traversing through such a medium. When two

waves with a phase difference $\Delta\Phi$ interfere, the number of intensity maxima and minima, M, is calculated as

$$M = \frac{\Delta\Phi}{2\pi} \tag{5}$$

For glass, this phase difference is determined by

$$\Delta\Phi(\theta) = 2\pi \frac{D}{\lambda_{\text{vac}}} \frac{n-1}{2n} \theta^2 \tag{6}$$

where D is the glass thickness, λ_{vac} is the wavelength in vacuum, and θ is the angle of incidence in radians. For glass plates pre-tilted at angles θ_1 and θ_2, the equation (6) modifies to

$$\Delta\Phi(\theta) = 2\pi \frac{D}{\lambda_{\text{vac}}} \frac{n-1}{2n} [(\theta + \theta_1)^2 - (\theta + \theta_2)^2]. \tag{7}$$

Similar to Equation (6), the phase difference for a gas is represented by

$$\Delta\Phi = 2\pi \frac{L}{\lambda_{\text{vac}}} (n-1)$$

where L denotes the length of the gas chamber. Additionally, the refractive index of an ideal gas can be approximated using the Lorentz-Lorenz law, which relates it to the gas's pressure p and temperature T. The Lorentz-Lorenz formula is expressed as

$$\frac{n^2-1}{n^2+1} = \frac{Ap}{RT} \tag{8}$$

where R denotes the universal gas constant and A represents the molecular refractivity of the gas.

3 Experimental Setup and Measurements

In this experiment, a Sagnac interferometer is utilized for the measurements. This type of interferometer is especially stable compared to other types of interferometers, such as the Mach-Zehnder or Michelson interferometer, due to both beams following the same path.

The Sagnac interferometer used in this experiment is schematically depicted in Figure 2. A Helium-Neon Laser, emitting light at a wavelength of $\lambda_{\text{Laser}} = 632.99\,\text{nm}$, serves as the coherent light source. The laser beam, after being reflected by adjustment mirrors M1 and M2, traverses a polarization filter before being split by the PBSC, as detailed in Section 2.1. The polarization filter regulates the intensities of the s- and p-polarized beams emitted from the PBSC. An equal intensity for both beams is achieved at a 45° angle of the polarization filter. The beams, one following a clockwise path and the other counter-clockwise, are then reflected by mirrors Ma, Mb, and Mc. They re-converge at the PBSC to form the output beam, which is split by another PBSC to be able to measure the s- and p-polarized parts of the beam separately.

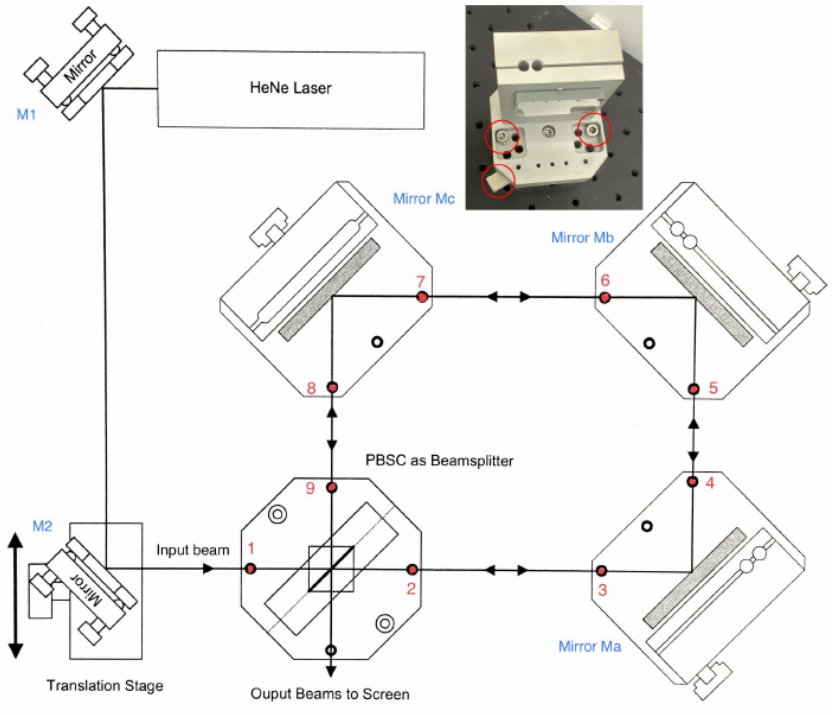

Figure 2: Schematic representation of the Sagnac interferometer setup. [3]

3.1 Alignment of the Sagnac Interferometer

The initial step in aligning the Sagnac Interferometer involves centering the laser beam on mirrors M1 and M2. These mirrors are crucial for directing the beam precisely through the center of the PBSC. Utilizing adjustment plates, the beam path is fine-tuned so that the laser strikes mirrors Ma and Mc centrally. Subsequent adjustments ensure both beams converge at the center of mirror Mb. Proper alignment is indicated when both beams rejoin in the PBSC. The quality of this alignment is gauged by observing the interference pattern of the output beam, with the polarization filter set to 45°. The presence of fringes in this pattern signals phase differences due to path variations, necessitating further adjustments to ensure the beams are perfectly parallel throughout the entire interferometer.

3.2 Measurement of the Contrast

To assess the contrast of the interference pattern, a rotating glass plane holder is positioned within the beam's path. The contrast is measured as a function of the polarization angle, varying the direction of the polarization filter in 5° increments across a range of 0° to 180°. A diode, by recording the voltage, measures the intensities of the minima and maxima in the interference pattern. Fine-tuning of these minima and maxima is achieved through adjustments made to the rotating glass plane holder.

For subsequent measurements, the polarization filter is set to an angle that maximizes the contrast, ensuring optimal conditions for accurate data collection.

3.3 Measurement of the Refractive Index of Glass

The refractive index of glass is measured using two diodes connected to a Modern Interferometry Controller. This device is designed to count the occurrences of intensity minima and maxima. The procedure involves gradually rotating the glass holder from 0° to 8°, and at each 2° increment, the count of maxima is recorded.

3.4 Measurement of the Refractive Index of Gas

The refractive index of air in the laboratory is determined as a function of pressure. A gas cell, with a length of $L = (100.0 \pm 0.1)\,\mathrm{mm}$, is inserted into the beam path to facilitate this measurement. Starting from a vacuum, the pressure inside the cell is incrementally increased. The count of intensity minima and maxima is recorded in steps of 50 mbar.

4 Analysis

Given that all angles in this study are measured in degrees, it is essential to convert them into radians for the purposes of trigonometric calculations mentioned in section 2. This conversion is achieved using the following formula:

$$\theta_{\mathrm{rad}} = \frac{2\pi}{360^\circ} \cdot \theta_{\mathrm{deg}}, \tag{9}$$

where θ_{deg} represents the angle in degrees and θ_{rad} denotes the angle in radians.

4.1 Determination of the Contrast in dependency of the polarisation angle

As described in Section 3.2, the minimum and maximum intensities for different polarization angles are measured. The measured values are listed in Table 1.

These values are used to calculate the contrast K for both sets of measurements using Equation (2). Subsequently, the mean and the standard deviation of K are computed using *numpy* [6]. Figure 3 visualizes these values of K.
For the fit, the function described in Equation (4) is modified by introducing a constant offset angle δ and a factor K_0 which represents the maximal contrast. Both parameters are allowed to vary in the fit to compensate for deviations between the experimental setup and the theoretical model. The resulting function is

$$K = 2K_0 |\sin(\phi - \delta)\cos(\phi - \delta)| \tag{10}$$

The fit, conducted using *scipy* [5], is displayed in Figure 3. The values of the parameters are

$$K_0 = 0.895 \pm 0.015 \quad \text{and} \quad \delta = (2.27 \pm 0.33)^\circ.$$

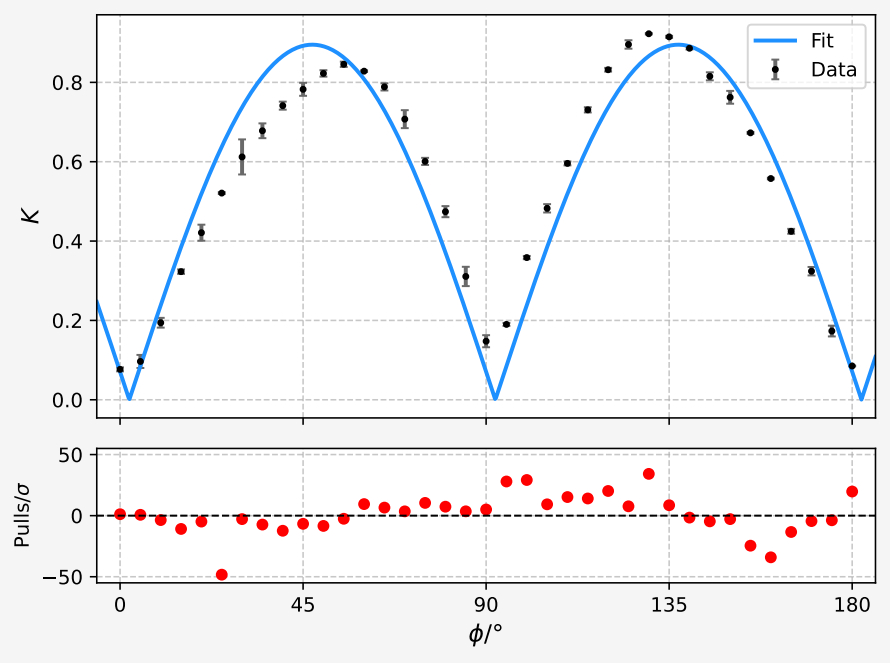

Figure 3: Averaged contrast K as a function of the polarization angle ϕ with a fit using the function described in Equation (10).

The maximum contrast was measured at a polarization angle of $\phi = 130°$. Henceforth, the polarization angle is set to this value for subsequent measurements.

4.2 Determination of the Refractive Index of Glass

For the measurement of the refractive index, two glass plates are placed into the beams of the interferometer as described in Section 3.3. Since the glass plates are tilted by $\theta_0 = \pm 10°$, Equation (7) can be simplified with $\theta_1 = -\theta_2 = 10°$ to

$$\Delta\Phi(\theta) = 2\pi \frac{D}{\lambda_{\text{vac}}} \frac{n-1}{n} \cdot 2\theta_0\theta. \tag{11}$$

This, combined with the relation (5), results in

$$M = \frac{D}{\lambda_{\text{vac}}} \frac{n-1}{n} \cdot 2\theta_0\theta \tag{12}$$

with the wavelength $\lambda = 632.99\,\text{nm}$ of the laser and the thickness $D = 1\,\text{mm}$ of the glass planes.

Table 2 shows the measured values for M at different angles θ. Equation (12) is fitted to the average M of all measured number of maxima, varying the parameter n. Figure 4 displays the fit to the mean values of M with the standard deviation represented as error bars. The fit yields a value of

$$n = (1.485 \pm 0.013)$$

$\phi/^\circ$	$I_{\mathrm{min1}}/\mathrm{V}$	$I_{\mathrm{max1}}/\mathrm{V}$	$I_{\mathrm{min2}}/\mathrm{V}$	$I_{\mathrm{max2}}/\mathrm{V}$
0	2.02	1.75	2.12	1.80
5	1.82	1.55	1.92	1.53
10	1.82	1.26	1.87	1.23
15	1.91	0.99	1.88	0.95
20	1.73	0.74	1.78	0.69
25	1.64	0.52	1.63	0.51
30	1.59	0.33	1.56	0.43
35	1.51	0.27	1.51	0.31
40	1.55	0.22	1.61	0.25
45	1.61	0.18	1.51	0.20
50	1.73	0.16	1.76	0.18
55	1.88	0.15	1.94	0.17
60	2.05	0.19	2.10	0.20
65	2.26	0.28	2.31	0.26
70	2.37	0.37	2.19	0.41
75	2.34	0.60	2.31	0.56
80	2.50	0.86	2.38	0.88
85	2.47	1.37	2.45	1.22
90	2.31	1.77	2.25	1.62
95	2.65	1.79	2.58	1.77
100	3.23	1.54	3.27	1.53
105	3.77	1.28	3.68	1.32
110	4.12	1.06	4.13	1.03
115	4.50	0.72	4.63	0.70
120	5.18	0.49	5.28	0.47
125	5.89	0.29	5.73	0.35
130	6.09	0.24	6.07	0.25
135	5.87	0.27	6.03	0.26
140	5.95	0.37	5.96	0.35
145	5.75	0.55	5.65	0.61
150	5.46	0.68	5.71	0.83
155	5.00	0.97	5.12	1.01
160	4.64	1.31	4.69	1.34
165	3.72	1.48	3.78	1.55
170	3.21	1.60	3.29	1.72
175	2.47	1.79	2.70	1.85
180	2.12	1.79	2.15	1.81

Table 1: Measured minimal and maximal intensity for different polarisation angles ϕ.

for the refractive index of the glass plates.

$\theta/°$	M_1	M_2	M_3	M_4	M_5	M_6	M_7	M_8	M_9	M
2	6	5	7	5	7	6	7	8	9	6.7 ± 1.2
4	12	9	13	13	13	11	11	15	14	12.3 ± 1.7
6	19	15	21	16	20	17	20	22	20	18.9 ± 2.2
8	27	16	25	23	24	25	25	26	25	24.0 ± 3.0
10	33	22	36	36	33	35	33	34	33	32.8 ± 4.0

Table 2: Measured values of the number of maxima M_i that passed the center for different angles θ and the calculated average M with standard deviation.

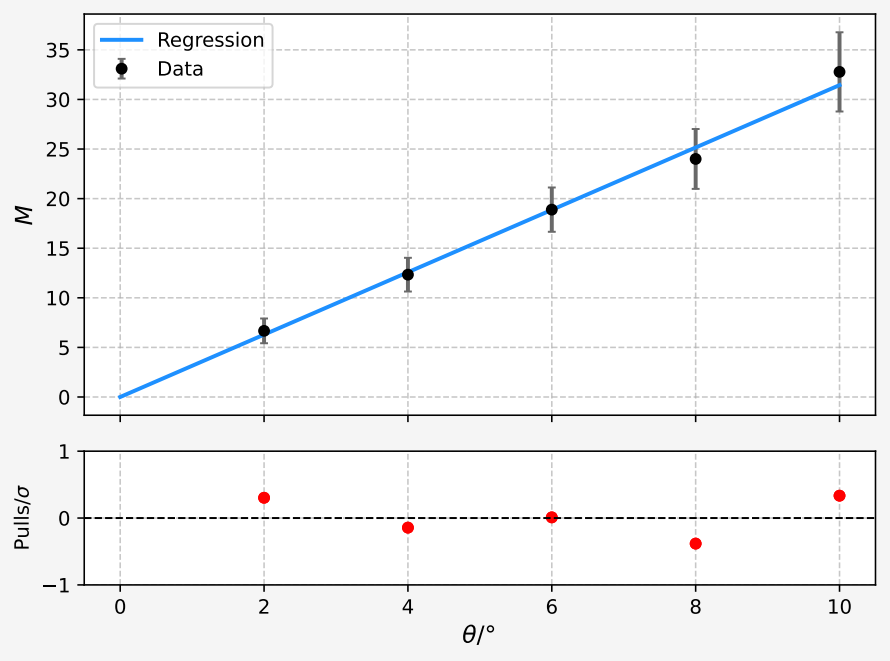

Figure 4: Averaged number of maxima M as a function of the angle θ with a fit using the function described in Equation (12).

4.3 Determination of the Refractive Index of Gas

The measured values for the number of maxima M that passed the center for different pressures are listed in Table 3. Figure 5 visualizes the averaged values of M as a function of the pressure p.

In the case where $n \approx 1$, the Lorentz-Lorenz law (8) can be simplified to

$$n = \frac{3}{2}\frac{Ap}{RT} + 1. \tag{13}$$

With the measured room temperature $T_{\text{room}} = 21.8\,°\text{C}$ and $L = (100.0 \pm 0.1)\,\text{mm}$, this results in a linear function

$$n(p) = \frac{3}{2}\frac{p}{RT_{\text{room}}} \cdot a + b \tag{14}$$

where the parameters a and b are fitted to the data. The fit is shown in Figure 5. The values of the parameters are

$$a = 4.44 \pm 0.02 \quad \text{and} \quad b = 0.999\,998\,7 \pm 0.000\,000\,8.$$

Plugging these values into Equation (13) with a temperature of $T = 15\,°\text{C}$ and a pressure of $p = 1013\,\text{hPa}$ leads to the measured refractive index of air at standard atmospheric conditions:

$$n_{\text{gas}} = (1.000\,273\,4 \pm 0.000\,001\,5)$$

p/mbar	M_1	M_2	M_3	M_4	M_5
50	2	1	2	2	2
100	4	3	4	4	4
150	6	6	6	7	7
200	9	8	9	9	9
250	11	10	11	11	11
300	13	12	13	13	13
350	15	14	15	15	15
400	17	16	18	17	17
450	19	18	20	19	19
500	21	20	22	21	21
550	23	22	24	23	23
600	25	25	26	25	26
650	28	27	29	28	28
700	30	29	31	30	30
750	32	31	33	32	32
800	34	33	35	34	34
850	36	35	37	36	36
900	38	37	40	38	38
950	40	40	43	40	41
1000	43	42	45	43	43

Table 3: Measured values of the number of maxima M that passed the center for different gas pressures p.

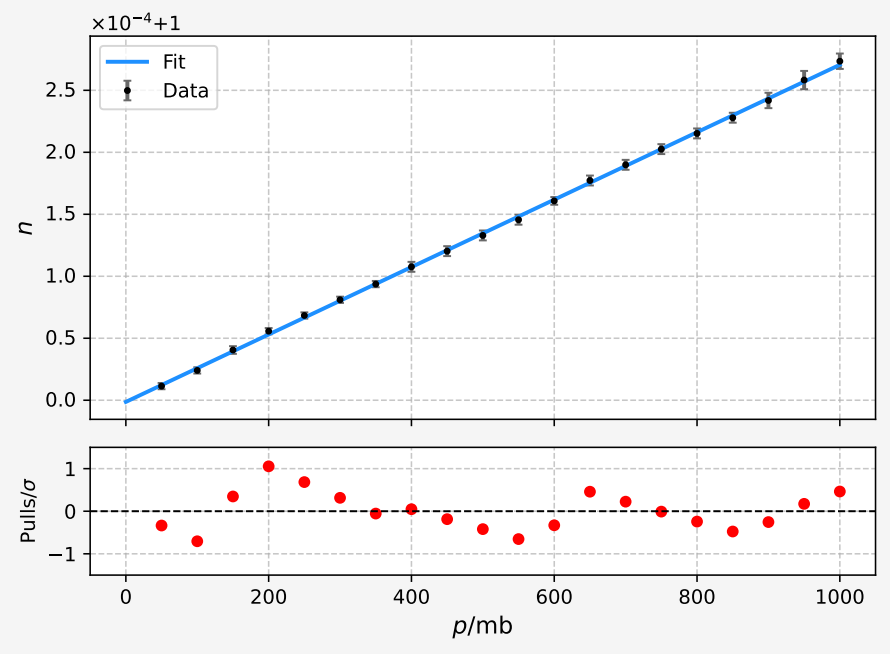

Figure 5: Averaged number of maxima M as a function of the gas pressure p with a fit using the function described in Equation (14).

5 Discussion

The contrast measurement yielded values within the expected range. The offset angle of $\delta = (2.27 \pm 0.33)°$ could be attributed to a constant offset in the polarizer or an offset in the laser's polarization angle. The amplitude of the contrast function, $K_0 = 0.895 \pm 0.015$, being below the theoretical value of one, suggests an imperfect alignment of the interferometer.

A notable issue in the measurement was fitting the theoretical function (10) to the data. The high residuals, reaching up to $50\,\sigma$, indicate that either the uncertainties were underestimated or that the theory does not fully account for certain effects present in the data. Given the challenges in measuring I_{min} and I_{max}, such as the sharp intensity distribution and intrinsic systematic uncertainties of the measuring device, which caused fluctuations during the measurement, it is plausible that the uncertainties in the fit are larger than estimated. This would, in turn, reduce the magnitude of the residuals.

The refractive index of glass was measured to be $n = 1.4850 \pm 0.0013$. Due to the variety of glass types and the unknown specific type of glass examined, a direct comparison with literature values is not feasible. However, most types of glass have a refractive index ranging between 1.4 to 1.9 [2], which is consistent with our measurement.

The refractive index of the gas in the room, under standard atmospheric conditions, was determined to be $n_{\text{gas}} = 1.000\,273\,4 \pm 0.000\,001\,5$. The literature value for air under standard conditions is $n_{\text{air}} = 1.000\,29$ [4]. While the deviation is small, it is significant due to the low uncertainty. However, this deviation can be explained by the unknown

exact composition of the gas in the room and the humidity levels.

References

[1] Rocky Mountain Instrument Co. *Polarizing Cube Beamsplitters*. http://rmico.com/polarizing-cube-beamsplitters.

[2] Wikipedia contributors. *List of refractive indices — Wikipedia, The Free Encyclopedia*. [Online; accessed 2023-12-19]. 2023. URL: https://en.wikipedia.org/wiki/List_of_refractive_indices.

[3] TU Dortmund. *V64 - Interferometry*. 2023.

[4] HyperPhysics. *Index of Refraction of Various Substances - HyperPhysics*. [Online; accessed 2023-12-19]. 2023. URL: http://hyperphysics.phy-astr.gsu.edu/hbase/Tables/indrf.html.

[5] Eric Jones, Travis E. Oliphant, Pearu Peterson, et al. *SciPy: Open source scientific tools for Python*. Version 0.16.0. URL: http://www.scipy.org/.

[6] Travis E. Oliphant. "NumPy: Python for Scientific Computing". Version 1.9.2. In: *Computing in Science & Engineering* 9.3 (2007), pp. 10–20. URL: http://www.numpy.org/.